



# Dependencies of Kappa Parameter on the Core Energy of Kappa Distributions and Plasma Parameter in the Case of the Magnetosphere of the Earth

I. P. Kirpichev<sup>1</sup> and E. E. Antonova<sup>2,1</sup>

<sup>1</sup> Space Research Institute, Russian Academy of Science, 84/32 Profsoyuznaya Str, 117997 Moscow, Russia; [ikir@iki.rssi.ru](mailto:ikir@iki.rssi.ru), [elizaveta.antonova@gmail.com](mailto:elizaveta.antonova@gmail.com)

<sup>2</sup> Federal State Budget Educational Institution of Higher Education, M. V. Lomonosov Moscow State University, Skobeltsyn Institute of Nuclear Physics (SINP MSU) Leninskie gory, GSP-1 119991 Moscow, Russia

Received 2019 December 3; revised 2020 January 23; accepted 2020 January 23; published 2020 March 2

## Abstract

Formation of kappa distribution functions and their relaxation to Maxwellian distributions are the main feature of astrophysical and space collisionless plasmas. In this work, we use the magnetosphere of the Earth as a giant plasma laboratory to study the properties of ion kappa distribution functions. Four years of measurements, performed by the multi-satellite *Time History of Events and Macroscale Interactions during Substorms (THEMIS)* mission during quiet geomagnetic conditions, at geocentric distances from three Earth radii ( $R_E$ ) to the magnetopause at daytime (of the order of  $10R_E$ ), and up to  $20R_E$  at night time are used for the analyses. We find a dependence of the  $k$  parameter on the core energy  $E_0$  of a single kappa distribution inside the magnetospheric ring current and in the plasma sheet, for different values of the plasma parameter (the ratio between the plasma and magnetic pressures). We show that  $k$  increases with  $E_0$  for all values of plasma parameter, which supports earlier results obtained for the magnetospheres of the Earth, Jupiter, and Saturn, but using lower statistics. However, contrary to previous results, our studies show that the relation between  $k$  and  $E_0$  is nonlinear, and most probably is a power law with a nearly constant index. The results obtained are relevant to solve the problem of thermalization of kappa distributions.

*Unified Astronomy Thesaurus concepts:* [Space plasmas \(1544\)](#); [Planetary magnetosphere \(997\)](#)

## 1. Introduction

The absence of coulomb collisions is typical in astrophysical and space plasmas. For example, the mean free path for coulomb collisions in the magnetosphere of the Earth is larger than the distance between the Sun and the Earth (Borovsky & Funsten 2003). However, despite this, the distribution functions have in general a comparatively regular shape. This means that the effectiveness of processes leading to the phase space relaxation should be very high. These processes include generation of waves, wave-particle and wave-wave interactions, suppression of phase space gradients, and particle acceleration leading to formation of power-law energetic tails of distribution functions. In most cases, the formed distribution functions are well fitted by kappa distributions, containing a Maxwellian core and a power-law tail. These kind of functions are commonly observed in astrophysical and space systems (see books of Bellan 2006; Binney & Tremaine 2008; and especially Livadiotis 2017). The kappa distribution is a basic function of nonextensive statistical mechanics that describes collisionless plasma systems, instead of the collisional systems described by Boltzmann-Gibbs statistics, and that arises from the interaction of turbulent wave fields with the particles far away from thermal equilibrium (Treuemann 2001). Determination of properties of kappa distribution functions and their evolution is important for many fields of astrophysics; taking into account that the power-law particle spectra are commonly observed in cosmic rays and the formation of power-law spectra has been analyzed in multiple works. A solution of the problem of formation and relaxation of kappa distributions requires the consideration of experimental results of the behavior of the collisionless plasma systems and theoretical analysis of nonlinear plasma interactions. The theory of formation of kappa distributions is still under development

(Yoon et al. 2006, 2012; Pierrard & Lazar 2010; Yoon 2012; Livadiotis 2015; Vafin et al. 2017), and the problem of relaxation of the kappa distribution to the Maxwellian one has not been properly studied yet. In the case of Maxwellian distributions, it is well known that the thermal equilibrium is a fundamental condition for their existence, but to date it is not clear what conditions are favorable for the formation and relaxation of kappa distributions.

Although the main properties of the kappa distribution functions were mainly obtained through solar wind studies (Leubner & Voros 2005; Leitner et al. 2009; Livadiotis et al. 2011, 2012, 2013, 2018), it is important to mention that kappa approximations were initially used for the analysis of plasmas in the Earth's magnetosphere (see the historical part of Livadiotis 2017). Interesting experimental results were related precisely to the solution of the problem of relaxation of kappa distributions. In particular, using the results of analyses of ion distributions in the solar wind (Collier et al. 1996) and the magnetospheres of the Earth (Christon et al. 1989), Jupiter (Collier & Hamilton 1995), and Saturn (Krimigis et al. 1983; Collier 1999), it was shown that the core energy (core temperature) of the kappa distribution  $E_0$  increases with the value of the kappa parameter  $k$ , using linear approximations. Collier (1999) suggested that these dependencies are the result of time-evolution of the distribution function, and developed a simple model of phase space diffusion with a constant diffusion coefficient. However, the aforementioned dependencies were obtained using small numbers of approximated spectra and did not consider the possible influence of the main plasma parameter  $\beta$ . This parameter is defined as the ratio between the plasma ( $p$ ) and the magnetic ( $B^2/2\mu_0$ ) pressures, where  $B$  is the magnetic field and  $\mu_0$  is the magnetic permeability of vacuum. Taking into consideration that  $\beta$  determines the development of all plasma processes, it is reasonable to assume

that the relaxation of kappa distributions to Maxwell distributions should also depend on this parameter. However, these studies have not been done yet.

The magnetosphere of the Earth is like a giant natural laboratory to study collisionless plasma phenomena, from which large series of particle spectra have been accumulated during the last decades using the measurements of multi-satellite missions. This laboratory has an important advantage in comparison to conventional laboratories: the size of the instruments are very small in comparison to the size of the measured structures. Differently to the solar wind, the flow velocities of ions are small in comparison to their thermal speed, and distribution functions are nearly isotropic especially during geomagnetically quiet periods. That is why the magnetosphere of the Earth represents a collisionless plasma system, which is very convenient for the study of relaxation of kappa distributions. It contains comparatively stable regions with very low and very high values of the plasma parameter  $\beta$ . The region of traditional ring current at geocentric distances  $<5R_E$  has very low  $\beta$  due to the high value of the Earth's magnetic field. It contains energetic ions and electrons with core energies  $\sim 50\text{--}100$  keV and energetic power-law tails. This region is also filled by cold plasma of ionospheric origin (plasmasphere) with high density in comparison to the density of the hot population. The lobes of the geomagnetic tail are also low  $\beta$  regions, but in contrast to the ring current, they have very low plasma density. The plasma sheet is a region of high  $\beta$  at geocentric distances  $>10R_E$ . A transition from low  $\beta$  to high  $\beta$  is observed at geocentric distances from 5 to  $7R_E$ . The main feature of the magnetic field at geocentric distances from 7 to  $10R_E$  is a day–night asymmetry. Due to compression of the geomagnetic field by the solar wind, the minimal values of magnetic field are shifted from the equator to higher latitudes. That is why high values of plasma  $\beta$  are observed near to the equatorial plane near midnight and at large  $Z_{GSM}$  near noon (Antonova et al. 2014). According to Antonova et al. (2018), this region is the outer part of the ring current, and is mapped to the main part of the auroral oval.

Kappa approximations were successfully used for magnetospheric studies by many researchers during both quiet and disturbed geomagnetic conditions (Christon et al. 1989, 1991; Pisarenko et al. 2002; Viñas et al. 2005; Runov et al. 2015; Stepanova & Antonova 2015; Kirpichev et al. 2017). A statistical distribution of the parameters of kappa functions during quiet time, expansion, and recovery phases of substorms was obtained by Espinoza et al. (2018). However, the parameters of kappa distributions were analyzed only in the midnight sector from 7 to  $30R_E$ ,  $X_{GSM} < 0$ ,  $|Y_{GSM}| < |X_{GSM}|$ , and  $|Z_{GSM}| < 8R_E$ . Nevertheless, none of these works were dedicated to studying a possible relation between the  $k$  index, the core energy ( $E_0$ ), and the plasma parameter.

In this paper we present the results of modeling ion spectra with kappa distribution functions during quiet geomagnetic conditions. We use ion flux measurements carried out by five satellites of the *THEMIS* mission in different regions of the magnetosphere of the Earth, and show how the plasma parameter affects the relation between the  $k$  index and the core energy. The paper is organized as follows: Section 2 contains instrumentation and data analysis, while the next two sections contain a detailed discussion of the dependence of  $k$  index on the core energy, and the conclusions.

## 2. Instrumentation and Data Analysis

For this study we used data of five satellites from the *THEMIS* mission between 2007 April and 2011 February (Angelopoulos 2008; Sibeck & Angelopoulos 2008). The ion spectra were obtained by combining the measurements of the Electrostatic Analyzer (ESA; McFadden et al. 2008) and the Solid State Telescope (SST; Angelopoulos 2008), using time and energy interpolation programs developed by the *THEMIS* team as part of the freely distributed TDAS/SPEDAS software. We used the data obtained when both the ESA and the SST instruments worked with maximum energy and angle resolution (full mode). The typical time was a few minutes with a cutoff equal to 10 minutes. The *THEMIS* instruments do not include a mass-spectrometer, and do not allow us to discriminate between ions of different species. However, it is well known that during the quiet time intervals, the  $H^+$  ions are dominant (Daglis et al. 1999). Only very quiet time intervals were selected according to the following criteria for Dst and auroral indexes:  $|Dst| < 20$  nT and  $|AL| < 300$  nT. This allows us to assume that protons make the main contribution to the ion spectra. Determination of the main plasma parameter requires the knowledge of the magnetic field. For this purpose we used the data from the fluxgate magnetometer with a time resolution of 3 s (Auster et al. 2008).

The three-dimensional kappa distribution has the form

$$f_1(E; n_0, \kappa, E_0) = \frac{n_0 m_p^{3/2}}{(2\pi E_0 \kappa)^{3/2}} \frac{\Gamma(\kappa + 1)}{\Gamma(\kappa - 1/2)} \cdot \left[ 1 + \frac{E}{\kappa E_0} \right]^{-\kappa-1}, \quad (1)$$

where  $n_0$  is the ion density,  $m_p$  is the mass of the particle,  $E = m_p V^2/2$  is the kinetic energy,  $E_0$  is the core energy,  $\Gamma$  is the Euler gamma function, and  $\langle E \rangle = 3E_0 k / (2(k - 3/2))$  is the mean energy (Livadiotis 2017).

For  $k \rightarrow \infty$  this function tends to the Maxwellian distribution:

$$f(E; n_0, E_0) = \frac{n_0 m_p^{3/2}}{(\pi E_0)^{3/2}} \exp\left(-\frac{E}{E_0}\right). \quad (2)$$

The spectra obtained for  $45^\circ\text{--}135^\circ$  pitch angles were fit by a single kappa distribution using a nonlinear least squares fitted with the Gradient-expansion algorithm adapted by the *THEMIS* team. Iterations were performed until the chi square changed by less than the convergence tolerance ( $=1.e-5$ ). Monte Carlo selection of input parameters was used. For the subsequent analysis we chose only the spectra well-fit according to the following criterion: the chi square should be less than 0.05.

Previous studies of ion spectra using *THEMIS* data (Stepanova & Antonova 2015; Espinoza et al. 2018) have shown that the main ion population can be fit by a single kappa function in a limited energy range (spectra between 1.75 and 210 keV were analyzed). Lower energies were discarded due to contamination from the spacecraft potential and photoelectrons, while higher energies were discarded due to contamination by energetic electrons and solar cosmic rays, and a low number of counts. However, in this study we did not fix the upper limit of energy. This limit was established individually for each spectrum in the following way: the spectrum in the full energy range is fit and the deviation between the fitted and measured spectrum for high-energy tail is analyzed. High-energy tail was

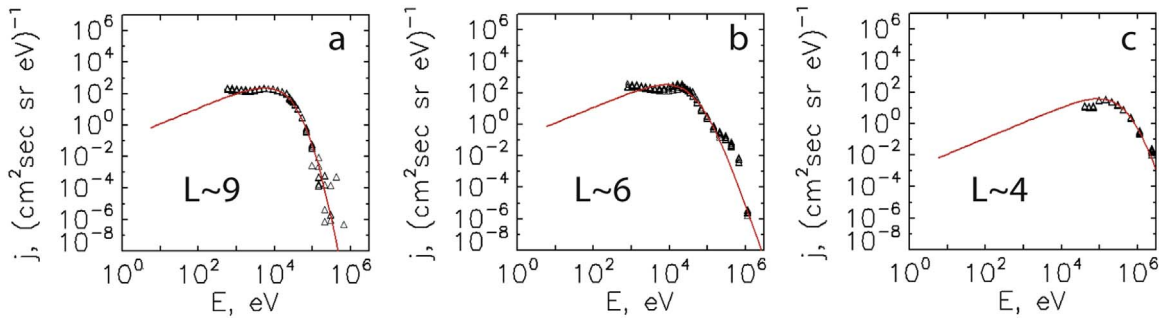


**Figure 1.** Examples of kappa approximations of measured spectra.

discarded if this difference was greater than twice the value of the fitted spectrum.

The orbits of all five *THEMIS* satellites are located near the equatorial plane covering the geocentric distances up to  $20R_E$ . This is convenient, if we consider that the parameters of the ion distribution functions are mainly controlled by processes near the minimum magnetic field, which is generally located near the equatorial plane. However, at the dayside the minimums are shifted away from the equatorial plane due to compression of the magnetic field. This effect leads to the splitting of the ring current into two branches, forming a high latitude continuation of the ordinary ring current, named cut-ring-current (CRC; see Antonova & Ganushkina 1997; Ganushkina et al. 2015, 2018; Antonova et al. 2018). This region is located at geocentric distances  $>7R_E$ . Therefore, at the dayside the ion spectra observed at the equatorial plane will be misidentified as spectra formed inside the low- $\beta$  region while they actually were formed inside the high- $\beta$  region, away from the equatorial plane (see the distribution of  $\beta$  parameter at the minimum  $\beta$  region in Antonova et al. 2014). The region at geocentric distances  $<5R_E$  corresponds to a low- $\beta$  region with a nearly dipolar magnetic field having its minimum values near the equatorial plane (the ring current domain). The region at geocentric distances  $>7R_E$  corresponds to a high- $\beta$  region, with minimum values close to the equatorial plane. The ions of ionospheric origin observed at the latitudes of the auroral oval at geocentric distances from 7 to 10  $R_E$  are difficult to recognize. The region between  $\sim 5$  and  $\sim 7R_E$  corresponds to  $\beta \sim 1$ . However, the observed ion spectra typically cannot be fitted by a single kappa distribution because of the action of local nonstationary processes like dispersionless injections (Lopez et al. 1990; Spanswick et al. 2010). Thus, the obtained statistics of single kappa approximations in this region are very low in comparison to the regions of low and high  $\beta$ .

Taking into account such features, we use the solar-magnetospheric (SM) coordinate system and select the sheet with thickness  $\pm 1R_E$  centered at  $Z_{SM} = 0$ . The dayside boundary of the analyzed region was established using the model of the magnetopause developed by Shue et al. (1998). The nightside boundary was located at  $20R_E$ . Using a cylindrical coordinate system with the origin at the Earth's center, we divided the data set into bins of  $0.5R_E$  in the radial direction, and  $10^\circ$  in azimuthal direction. The time of crossing of a bin by a single satellite is of the order of 10 minutes. This means that only a few spectra were considered during a single bin crossing. Next, for each bin the spectral fitted parameters were averaged, mixing fit results from all satellites. Figures 1(a)–(c) show examples of spectra fitted by single kappa distribution functions for measurements taken at geocentric

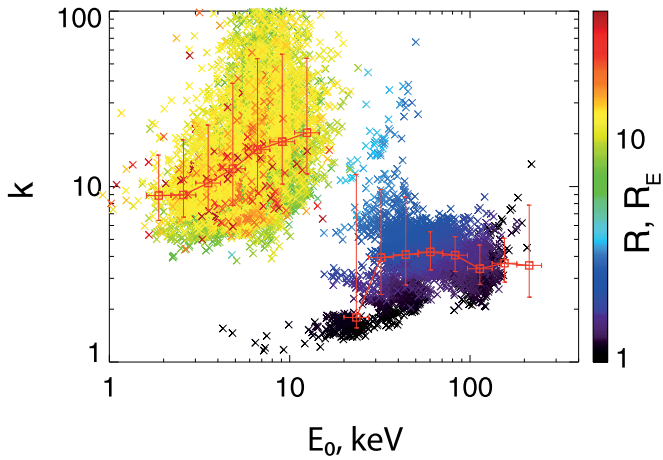
distances of  $\sim 9$ , 6 and  $4R_E$ , respectively. As it can be seen, the obtained fits differ significantly: the more energetic inner ring current ions ( $L \sim 4R_E$ ) have energetic rigid high-energy spectra, corresponding to low values of kappa, and high values for the core energy. On the other hand, at larger distances the spectra are softer and closer to Maxwellian ones.

Figure 2 shows the relation between  $k$  and  $E_0$  obtained using the measured spectra at all geocentric distances, as indicated by the color bar. Two subsets of spectra, corresponding to the near Earth (black–blue subset) and the tail (green–yellow subset), can be easily identified. The data were divided into energy bins equally spaced in logarithmic scale. For each bin we calculated the median kappa parameter and they are shown with red squares. The error bars correspond to standard deviations calculated independently for the values more and less than the median value. As it can be seen, the values of kappa increase with  $E_0$  for each subset, both for high- $\beta$  (large distances) and low- $\beta$  (ring current) regions.

Figure 2 shows that there is a significant difference in the values of  $E_0$  between the ring current region ( $R \lesssim 7R_E$ , very low  $\beta$ ) and the CRC and plasma sheet region ( $R \gtrsim 7R_E$ , high  $\beta$ ), meanwhile the number of spectra in the region where  $\beta \sim 1$  is low. This is related to the fact that  $\beta \sim 1$  plasma corresponds to an equatorial region mapped from the auroral oval. In this region there are two different sources of ion population. In addition to solar wind magnetospheric ions, ion beams, and conics of ionospheric origin are also frequently observed. Therefore, the ion distribution functions typically exhibit two maxima and cannot be fitted with a single kappa function. Figure 3 shows the relation between the median values of the  $k$  parameter in 20 logarithmically spaced bins of the  $\beta$  parameter. As it can be seen,  $k$  increases with  $\beta$  up to  $\beta \sim 1$ . For higher values of  $\beta$  the values of  $k$  are almost constant within the error bars, though a small decrease is noticeable.

As it can be seen from Figures 2 and 3, the values of kappa depend on both  $\beta$  and  $E_0$ . To unravel this tangle we divided the data set into six logarithmically spaced bins of  $\beta$  with the following central values:  $\beta = 0.001$  (black squares),  $=0.01$  (dark blue squares),  $=0.05$  (green squares),  $=0.1$  (yellow squares),  $=1$  (orange squares), and  $=10$  (red squares). Within each bin the data subsets were divided into bins of logarithmically spaced core energy  $E_0$ . Figure 4 shows the final dependence of  $k$  on  $E_0$  for different  $\beta$ . Subsequently, each curve was fitted with a power law of the form  $k = AE_0^\alpha$ , where  $A$  is the constant of fitting.

Table 1 summarizes the results of fitting  $k$  versus  $E_0$  with power-law functions. It is possible to see the increase of  $A$  and  $\alpha$  with  $\beta$ . However, in spite of the large range of  $\beta$  values



**Figure 2.** Dependence of  $k$  on  $E_0$  and geocentric distances, as shown by the logarithmic color-bar scale (in  $R_E$ ).

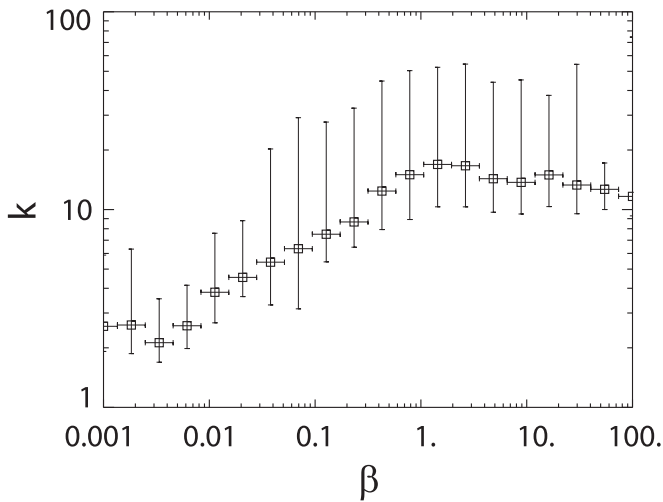


**Figure 3.** Integral dependence of the  $k$  parameter on the plasma  $\beta$ .

(orders of magnitude), the value of  $A$  changes less than a factor of 20, and the value of  $\alpha$  is practically constant, at around 0.5.

Figure 5 shows the comparison of fitting curves from Figure 4 with the results of fitting from Collier (1999). It is possible to see that our fits describe better the relation between  $E_0$  and kappa in comparison with earlier results. However, dependencies shown by Collier (1999) were obtained using a very small number of kappa fits. Therefore, we believe that our results do not contradict the results summarized by Collier (1999), who also discussed the possibility of nonlinear fits to the relation between  $k$  and  $E_0$ . The obtained dependencies show that the value of  $A$  weakly increases with  $\beta$  for a wide range of  $\beta$ . The most interesting feature is the practical independence of  $\alpha$  on  $\beta$ . Such independence could mean that the relaxation of ion kappa distributions to Maxwell distributions is a process weakly dependant on the properties of developed instabilities and spectra of generating waves, which will be difficult to explain. However, the error bars are large and in the future it will be interesting to analyze the existence of a universal law of the form  $k \sim E_0^{1/2}$ .

### 3. Discussion

We have analyzed the kappa  $k$  and core energy  $E_0$  values that were obtained from fits of ion spectra to single kappa

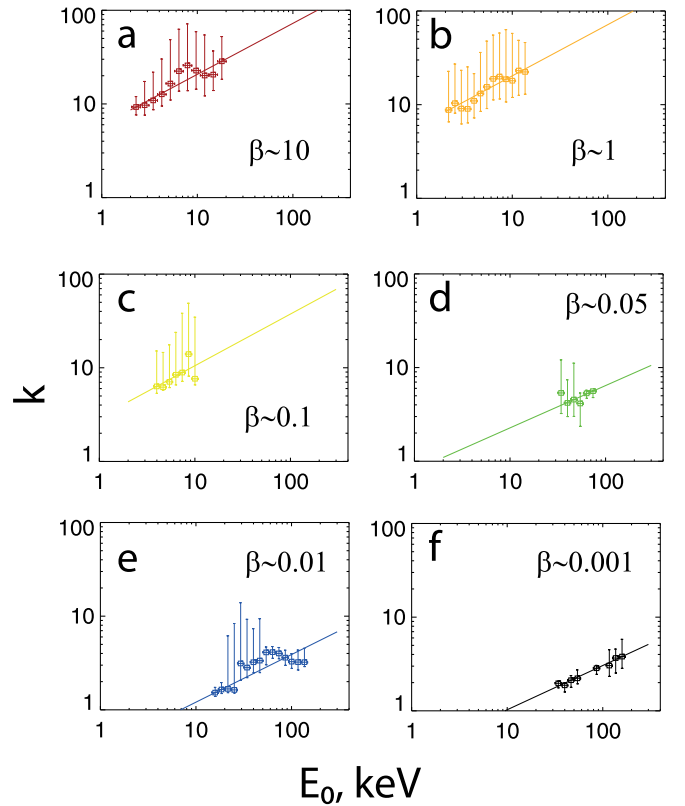


**Figure 4.** Dependence of  $k$  on  $E_0$  in the regions with different  $\beta$ . The central value of each  $\beta$  is indicated in each figure. The exact range is indicated in Table 1.

**Table 1**

Results of Fitting  $k$  versus  $E_0$  with Power-law Functions within a Restricted Range of Beta Values

$\beta$	$A$	$\alpha$
$0.001 \pm 0.004$	0.35	0.47
$0.01 \pm 0.005$	0.37	0.51
$0.05 \pm 0.025$	0.80	0.45
$0.1 \pm 0.06$	2.95	0.55
$1 \pm 0.5$	5.76	0.55
$10 \pm 8$	5.91	0.54

distribution functions in different regions of the magnetosphere of the Earth, and during very quiet geomagnetic conditions. Our study of a possible relation between the values of kappa and  $E_0$  showed that, in agreement with previous works, the values of  $k$  increase with  $E_0$  in different magnetospheric regions. The relation seems to be nonlinear and holds for regions with different magnetic fields, ion properties, and kappa parameters, but within a restricted range of beta values. This allowed us to analyze the  $k$  parameter increases during the evolution of kappa distributions to Maxwellian ones.

It is interesting to compare our results with solar wind ion kappa approximations, as they were obtained in very different conditions but show the same correlation (see Figure 1 in Collier 1999). Careful analysis of kappa parameters in the solar wind was recently produced by Livadiotis et al. (2018) at nearly one astronomical unit (a.u.). They used large statistics and showed that kappa distributions vary significantly with solar wind parameters, which gives the possibility to characterize possible mechanisms to generate kappa functions.

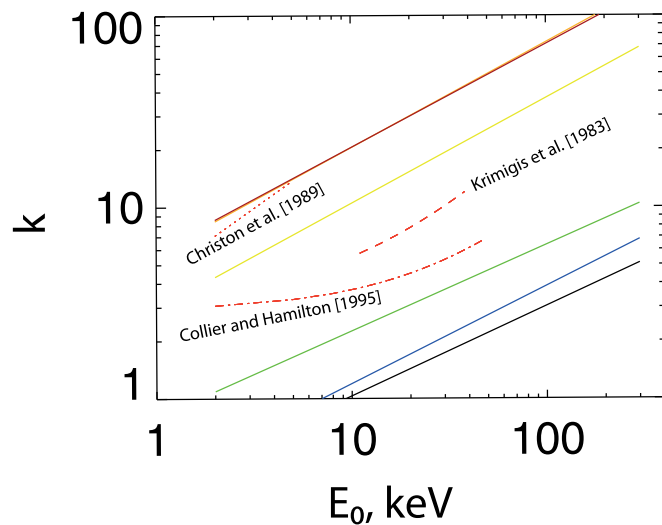


**Figure 5.** Comparison of our results in Figure 4 (continuous lines of the same color as in Figure 4), with the result of fits summarized by Collier (1999), which correspond to the geomagnetic tail (dotted red line; from Christon et al. 1989), to the magnetosphere of Jupiter (dashed-dotted line; from Collier & Hamilton 1995), and to the magnetosphere of Saturn (dashed line; from Krimigis et al. 1983).

Livadiotis et al. (2018) did not discuss the relation between  $k$  and  $E_0$ . However, they obtained a dependence of  $k$  on  $\beta$  (see Figure 10 of their paper), which qualitatively coincides with our results. A more detailed comparison is difficult due to different forms of presentation. Collier (1999) produced a simplified analysis of kappa distribution evolution in the process of Maxwellization and explained the increase of  $k$  with the increase of  $E_0$  as a result of phase space diffusion. He obtained a linear dependence for these quantities. Our analysis based on a large database shows the nonlinear character of this dependence, which requires careful analysis and explanation.

However, it is clear that the increase of  $k$ , which implies softening of the spectra, will lead to an increase of  $E_0$  if the energy of the most energetic particles is redistributed between core particles during the evolution of the kappa function, in the absence of acceleration and particle losses. It will be interesting to analyze such processes in the future.

#### 4. Conclusions

Using the magnetosphere of the Earth as a giant laboratory to study ion kappa distributions, we measured the kappa parameters for single kappa function approximations in different magnetospheric regions and during quiet magnetospheric conditions. The obtained approximations give the possibility of determining the dependency of the  $k$  parameter on the core energy  $E_0$  for a wide energy range and a wide range of the plasma parameter. Our results support earlier results that show that  $k$  increases with  $E_0$  in the solar wind and in the magnetospheres of the Earth, Jupiter, and Saturn. However, in contrast to previous analyses, our analysis shows a nonlinear dependence of  $k$  on  $E_0$ , which is better approximated by a power function. We suggest that the increase of  $k$  with the increase of  $E_0$  is a natural process of kappa distribution evolution to a Maxwellian one in the absence of particle acceleration and losses.

We show a clear dependence of  $k$  on plasma  $\beta$ . Kappa parameters increase with  $\beta$ . However, the slope of  $\log k$  versus  $\log E_0$  is practically independent of  $\beta$  and has the form

$\log k \sim 0.5 \log(E_0)$ , i.e.,  $k \sim E_0^{1/2}$ . Such dependence was obtained at quiet geomagnetic conditions and in very different plasma regions. Our results show that when plotting the theoretical kappa distribution (Leubner 2004) it is evident that changes in the kappa parameter correspond not only to changes in the suprathermal tail population but also in a redistribution of the core particles for one specific  $E_0$ .

We think that the obtained dependencies are a very important part of the dynamics of the relaxation of kappa distributions to Maxwell distributions and require a proper theoretical explanation.

The data of the *THEMIS* satellite mission used in this work are available at <http://themis.ssl.berkeley.edu/>, <http://cdaweb.gsfc.nasa.gov/>, and can also be downloaded via ftp from [http://themis.ssl.berkeley.edu/data\\_retrieval.shtml](http://themis.ssl.berkeley.edu/data_retrieval.shtml).

Software: SPEDAS 3.0 (Angelopoulos et al. 2019).

#### ORCID iDs

I. P. Kirpichev <https://orcid.org/0000-0002-9314-1325>  
E. E. Antonova <https://orcid.org/0000-0001-6980-3993>

#### References

- Angelopoulos, V. 2008, *SSRv*, **141**, 5  
 Angelopoulos, V., Cruce, P., Drozdov, A., et al. 2019, *SSRv*, **215**, 9  
 Antonova, E. E., & Ganushkina, N. Y. 1997, *JATP*, **59**, 1343  
 Antonova, E. E., Kirpichev, I. P., & Stepanova, M. V. 2014, *JASTP*, **115**, 32  
 Antonova, E. E., Stepanova, M. V., Kirpichev, I. P., et al. 2018, *JASTP*, **177**, 103  
 Auster, H. U., Glassmeier, K. H., Magnes, W., et al. 2008, *SSRv*, **141**, 235  
 Bellan, P. M. 2006, *Fundamentals of Plasma Physics* (Cambridge: Cambridge Univ. Press)  
 Binney, J., & Tremaine, S. 2008, *Galactic Dynamics* (2nd ed.; Princeton, NJ: Princeton Univ. Press)  
 Borovsky, J. E., & Funsten, H. O. 2003, *JGR*, **108**, 1284  
 Christon, S. P., Williams, D. J., Mitchell, D. G., Frank, L. A., & Huang, C. Y. 1989, *JGR*, **94**, 13409  
 Christon, S. P., Williams, D. J., Mitchell, D. G., Huang, C. Y., & Frank, L. A. 1991, *JGR*, **96**, 1  
 Collier, M. R. 1999, *JGR*, **104**, 559  
 Collier, M. R., & Hamilton, D. C. 1995, *GeoRL*, **22**, 303  
 Collier, M. R., Hamilton, D. C., Gloeckler, G., Bochsler, P., & Sheldon, R. B. 1996, *GeoRL*, **23**, 1191  
 Daglis, I. A., Thorne, R. M., Baumjohann, W., & Orsini, S. 1999, *RvGeo*, **37**, 407  
 Espinoza, C. M., Stepanova, M., Moya, P. S., Antonova, E. E., & Valdivia, J. A. 2018, *GeoRL*, **45**, 6362  
 Ganushkina, N. Y., Liemohn, M. W., & Dubyagin, S. 2018, *RvGeo*, **56**, 309  
 Ganushkina, N. Y., Liemohn, M. W., Dubyagin, S., et al. 2015, *AnGeo*, **33**, 1369  
 Kirpichev, I. P., Antonova, E. E., & Stepanova, M. 2017, *JGR*, **122**, 8078  
 Krimigis, S. M., Carbary, J. F., Keath, E. P., et al. 1983, *JGR*, **88**, 8871  
 Leitner, M., Voros, Z., & Leubner, M. P. 2009, *JGR*, **114**, A12104  
 Leubner, M., & Voros, Z. 2005, *ApJ*, **618**, 547  
 Leubner, M. P. 2004, *ApJ*, **604**, 469  
 Livadiotis, G. 2015, *JGR*, **120**, 880  
 Livadiotis, G. 2017, *Kappa Distribution: Theory Applications in Plasmas* (1st ed.; Amsterdam: Elsevier)  
 Livadiotis, G., Desai, M. I., & Wilson, L. B. 2018, *ApJ*, **853**, 142  
 Livadiotis, G., McComas, D. J., Dayeh, M. A., Funsten, H. O., & Schwadron, N. A. 2011, *ApJ*, **734**, 1  
 Livadiotis, G., McComas, D. J., Randol, B., et al. 2012, *ApJ*, **751**, 64  
 Livadiotis, G., McComas, D. J., Schwadron, N. A., Funsten, H. O., & Fuselier, S. A. 2013, *ApJ*, **762**, 134  
 Lopez, R. E., Sibeck, D. G., McEntire, R. W., & Krimigis, S. M. 1990, *JGR*, **95**, 109  
 McFadden, J., Carlson, C., Larson, D., et al. 2008, *SSRv*, **141**, 277  
 Pierrard, V., & Lazar, V. 2010, *SoPh*, **267**, 153  
 Pisarenko, N. F., Budnik, E. Y., Ermolaev, Y. I., et al. 2002, *JASTP*, **64**, 573  
 Runov, A., Angelopoulos, V., Gabrielse, C., et al. 2015, *JGR*, **120**, 4369

- Shue, J. H., Song, P., Russell, C. T., et al. 1998, [JGR](#), **103**, 17691
- Sibeck, D. G., & Angelopoulos, V. 2008, [SSRv](#), **141**, 35
- Spanswick, E., Reeves, G. D., Donovan, E., & Friedel, R. H. W. 2010, [JGR](#), **115**, A11214
- Stepanova, M., & Antonova, E. E. 2015, [JGR](#), **120**, 684
- Treumann, R. A. 2001, [Ap&SS](#), **277**, 81
- Vafin, S., Riazantseva, M., & Yoon, P. H. 2017, [ApJ](#), **850**, 78
- Viñas, A. F., Mace, R. L., & Benson, R. F. 2005, [JGR](#), **110**, A06202
- Yoon, P. H. 2012, [PhPl](#), **19**, 052301
- Yoon, P. H., Rhee, T., & Ryu, C. M. 2006, [JGR](#), **111**, A09106
- Yoon, P. H., Ziebell, L. F., Gaelzer, R., Lin, R. P., & Wang, L. 2012, [SSRv](#), **173**, 459